CSQCD V, l'Aquila 2016

Simulations of the Neutron Star Crust

- general remarks on NS and crust
- modeling approach
- nuclear matter and nuclei
- inner crust – pasta phase
- what's next

***R. Nandi**, SWS   FIAS Frankfurt*

structure of neutron star

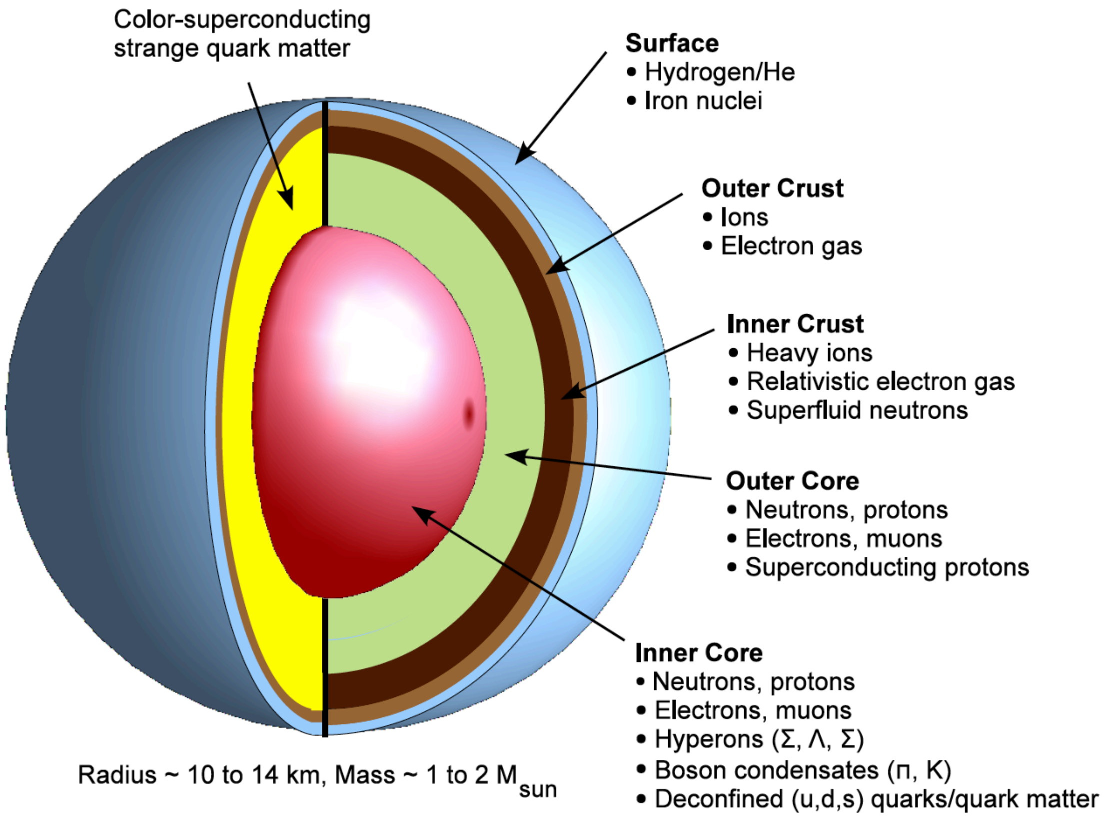

Weber et al, IJMPD 19, 1427 (2010)

structure of the crust

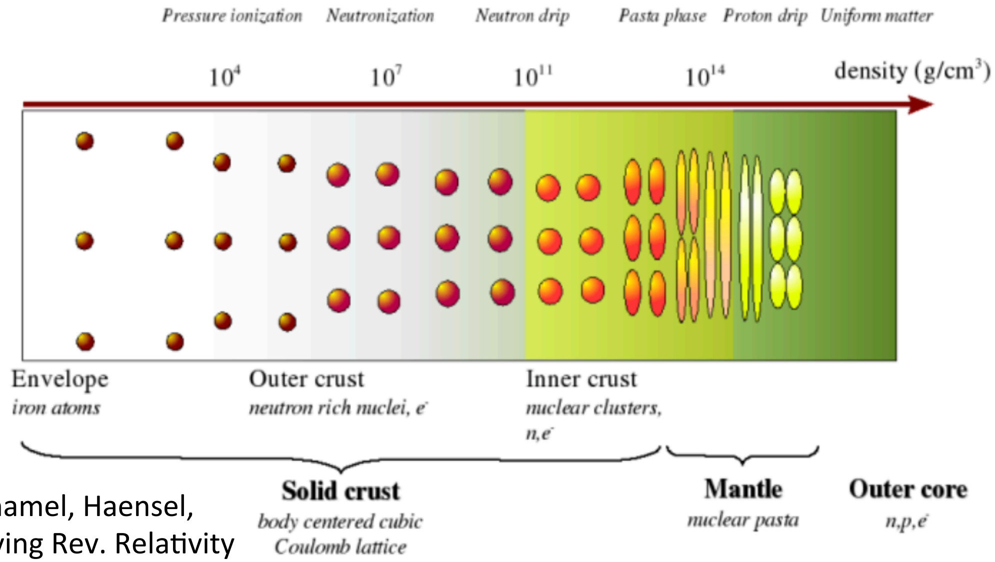

Chamel, Haensel, Living Rev. Relativity 11, 10 (2008)

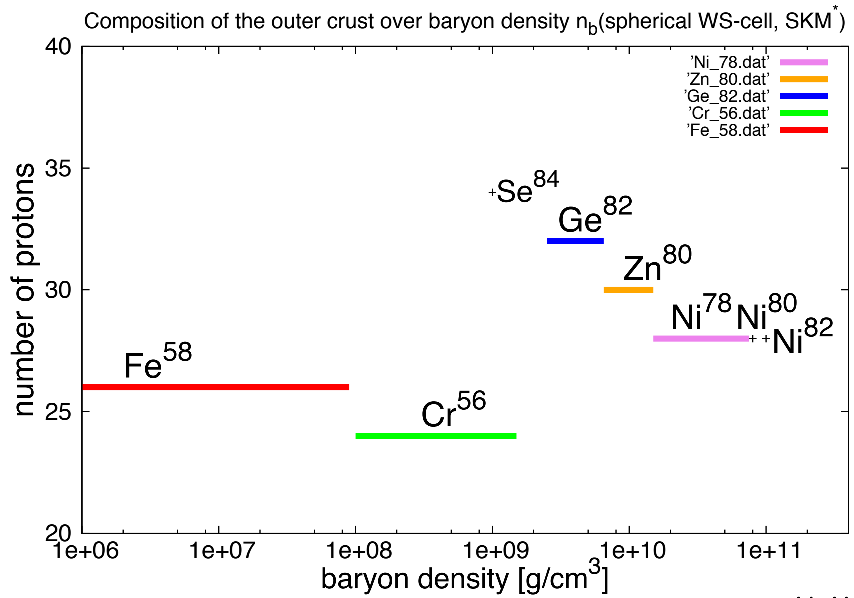

U. Heinzmann

non-accreting crust (BPS)

	ρ [g/cm³]
^{56}Fe	8.1×10^{6}
^{62}Ni	2.7×10^{8}
^{64}Ni	1.2×10^{9}
^{84}Se	8.1×10^{9}
^{82}Ge	2.2×10^{10}
^{80}Zn	4.9×10^{10}
^{78}Ni	1.6×10^{11}
^{76}Fe	1.8×10^{11}
^{124}Mo	1.9×10^{11}
^{122}Zr	2.7×10^{11}
^{120}Sr	3.7×10^{11}
^{118}Kr	4.3×10^{11}

results can be very model-dependent

see e.g. Rüster et al, PRC **73**, 035804 (2006) extreme example - total binding energy –B (MeV) for Uranium Isotopes

side remark - drip line for heavy nuclei highly uncertain (far beyond crust conditions)

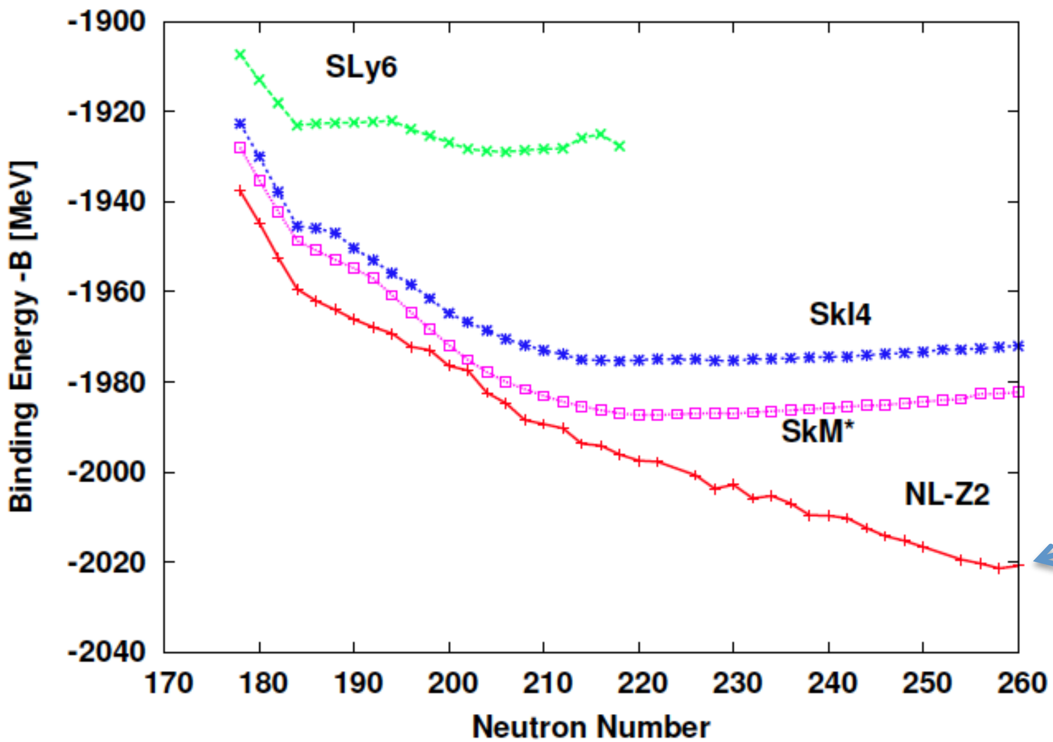

more parameter sets behave similarly

SWS,Gridnev,Tarasov,Tarasov,Geiner, IJMPE**21**, 1250047 (2012)

Model	N(1d)	N(2d)	B_{2d} [MeV]
NL-Z2	258	258	2021.34
SkM*	246	220	1987.39
SkI4	258	218	1975.41
SLy6	184	206	1928.92
χ_M	184	184	1957.56
χ_M*		224	1965.7

different Skyrme, RMF, CMF models

drip line nuclei 1d, 2d

new shell generates magic number at N = 258

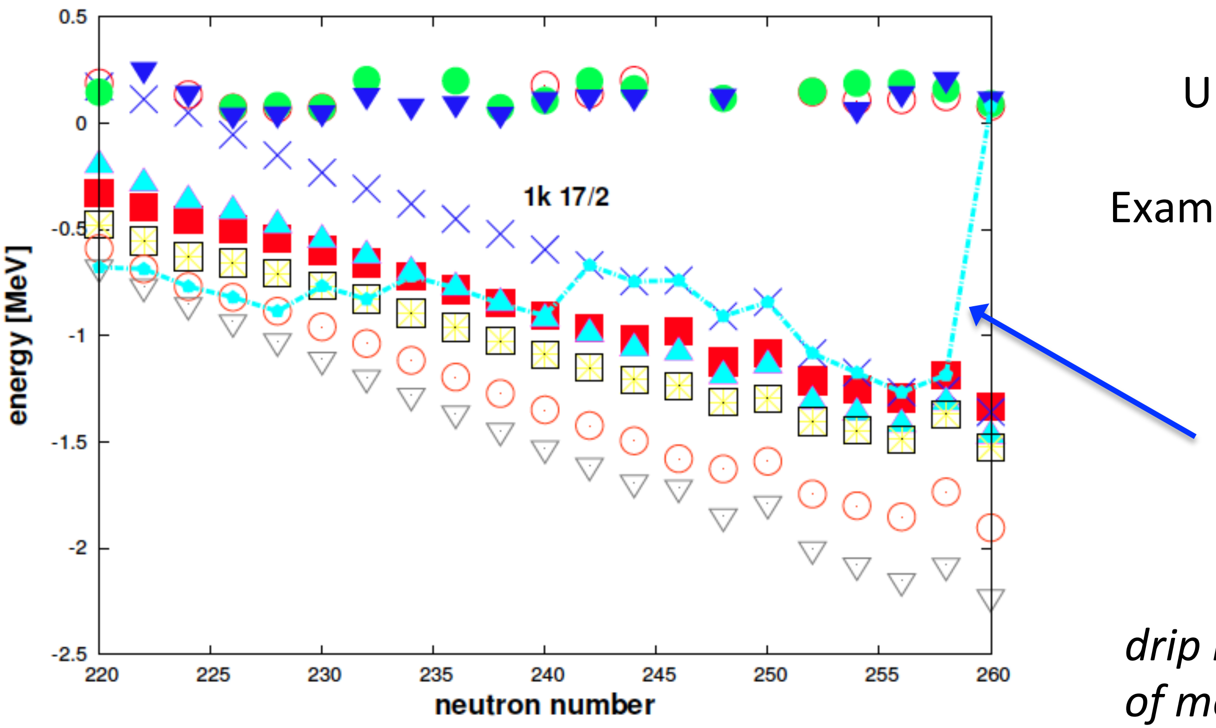

Uranium Isotopes

Example: NL-Z2 RMF

Fermi energy

drip line uncertainty of more than 70 neutrons!

outer crust - situation quite different for accreting neutron stars

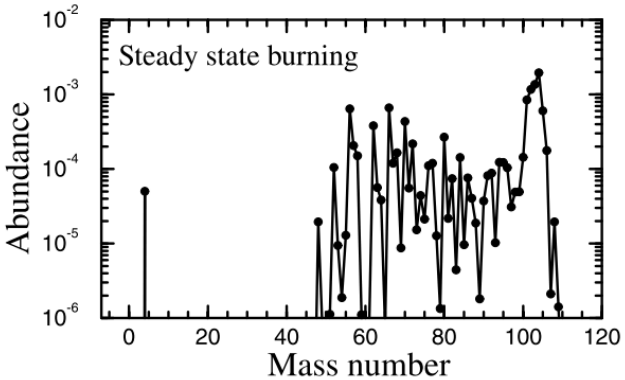

from Schatz et al, PRL 86, 3471 (2001)

rp process up to Z = 54 (Xe)

steady-state distribution sinks into crust
complex system close to drip line
with 18 different nuclei (Z <= 47)

Gupta et al, ApJ662,1188 (2007)

significant changes of transport properties
liquid-solid transition temperature changes
phase separation effects might lead to large C abundance
such complex systems require huge amount of statistics

Horowitz et al., Phys.Rev.E75 066101 (2007)

neutron star properties including rotation

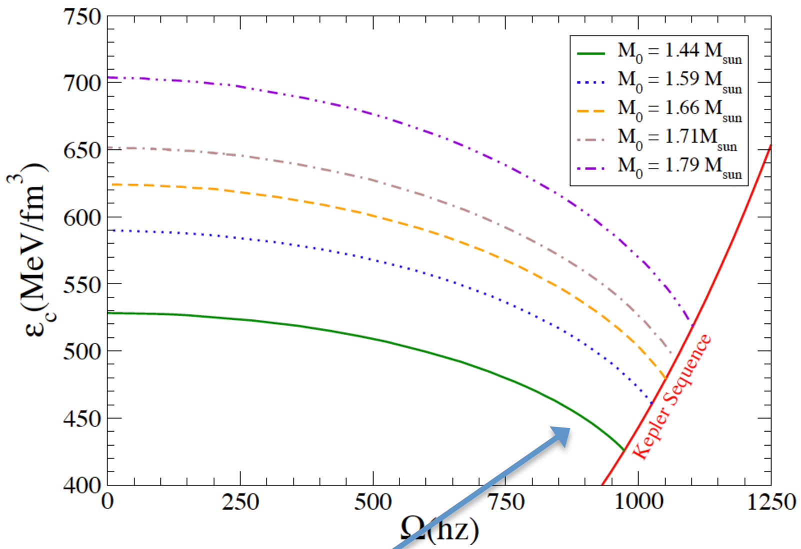

central energy density significantly reduced

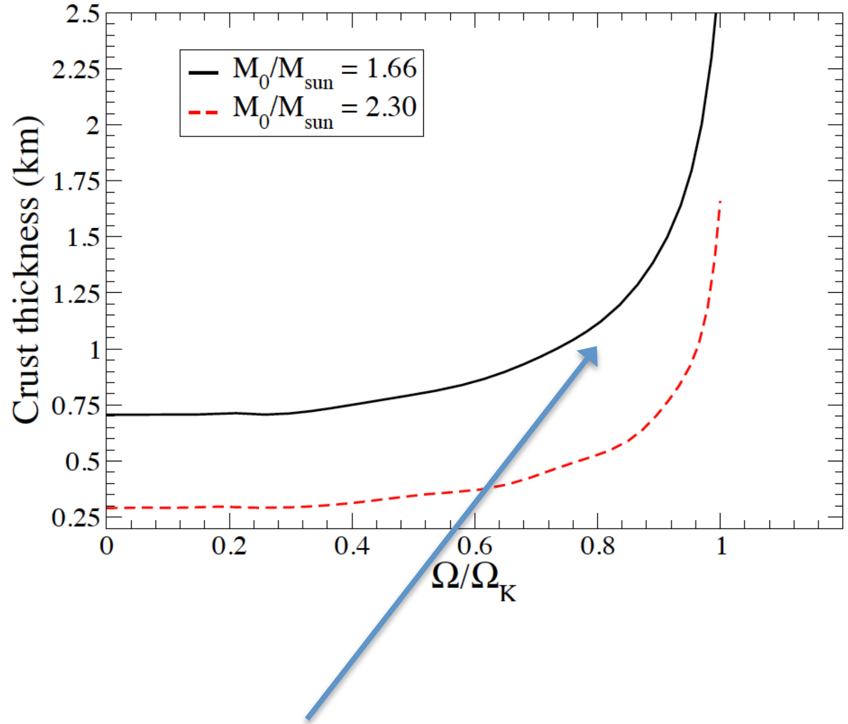

big change of crust thickness

Negreiros, Weber, SWS in "Neutron Star Crusts" (2012)

cooling in rotating stars

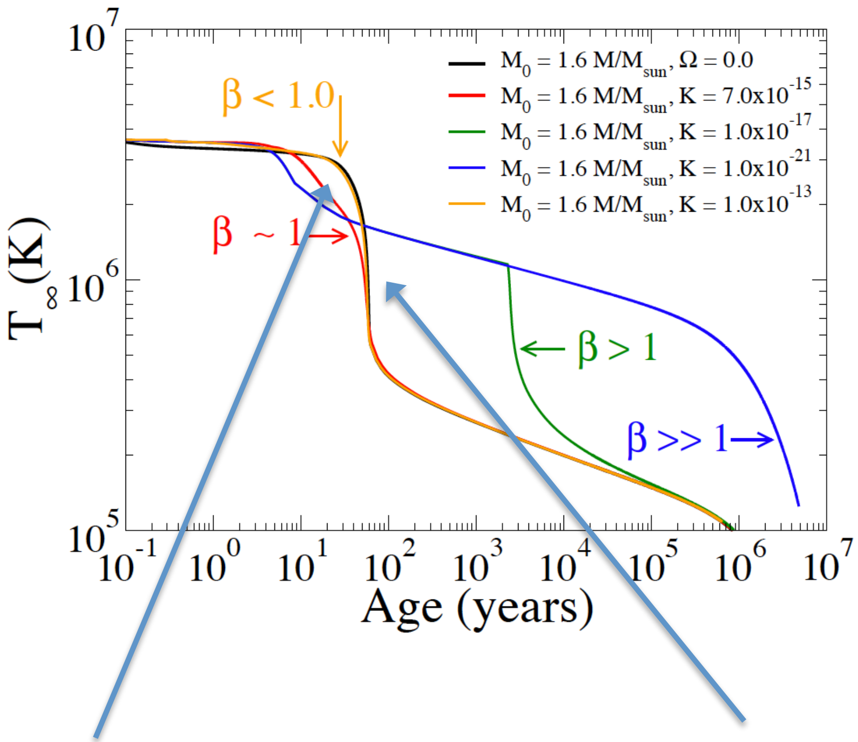

early core-crust coupling

cold wave reaches crust

fast cooling of the core (direct Urca)

β ratio of spin-down to cooling relaxation time

size of the crust might change during the evolution of the star

Negreiros, Weber, SWS PLB 718, 1176

simulating outer and inner crust

study crust properties using molecular dynamics techniques

several active groups

Horowitz et al. (MD, inner and outer crust)
Maruyama et al. (QMD, inner crust)
Dorso et al. (MD, inner crust)

inner crust – frustrated system
competition of attractive and repulsive forces
typically leads to many competing minima

large statistics, dynamical approach

→ develop GPU code

started out with atomic clusters, carbon nanotubes

Yakubovich, Sushko, SWS, Solovyov
PRB 88, 035438

Quantum molecular dynamics approach

Large-scale N-particle simulations

single particle – Gaussian wave packet

$$\phi_i(\mathbf{r}) = \langle \mathbf{r} | \phi_i \rangle = \frac{1}{(2\pi C_W)^{3/4}} \exp\left[\frac{-(\mathbf{r} - \mathbf{R_i})^2}{4C_W} + \frac{i}{\hbar} \mathbf{r} \, . \, \mathbf{P}_i \right]$$

N-particle wavefunction

$$|\phi\rangle = |\phi_1\rangle \otimes |\phi_2\rangle \otimes | \cdots \otimes |\phi_N\rangle$$

in analogy to molecular dynamics approaches
in simulations of heavy-ion simulations (e.g. UrQMD, …)

Aichelin, Stöcker, PLB 176, 14

general structure of Hamitlonian

$$\mathcal{H} = T + V_{\rm Pauli} + V_{\rm Skyrme} + V_{\rm sym} + V_{\rm MD} + V_{\rm Coul}$$

$$T = \sum_{i,j(\neq i)} \frac{\mathbf{P}_i^2}{2m_i}$$

Local interactions

$$V_{\rm Skyrme} = \frac{\alpha}{2\rho_0} \sum_{i,j(\neq i)} \rho_{ij} + \frac{\beta}{(1+\tau)\,\rho_0^{\tau}} \sum_i \left[\sum_{j(\neq i)} \tilde{\rho}_{ij} \right]^{\tau} ,$$

ρ_i, $\tilde{\rho}_i$ are single-nucleon densities and ρ_{ij}, $\tilde{\rho}_{ij}$ are overlap between nucleons

$$\rho_i(\mathbf{r}) = |\psi_i(\mathbf{r})|^2 = \frac{1}{(2\pi C_W)^{3/2}} \exp\left[-\frac{(\mathbf{r}-\mathbf{R}_i)^2}{2C_W}\right], \quad \tilde{\rho}_i(\mathbf{r}) = \frac{1}{(2\pi \tilde{C}_W)^{3/2}} \exp\left[-\frac{(\mathbf{r}-\mathbf{R}_i)^2}{2\tilde{C}_W}\right],$$

$$\rho_{ij} \equiv \int d^3\mathbf{r} \rho_i(\mathbf{r})\rho_j(\mathbf{r}) , \quad \tilde{\rho}_{ij} \equiv \int d^3\mathbf{r} \tilde{\rho}_i(\mathbf{r})\tilde{\rho}_j(\mathbf{r}), \qquad \tilde{C}_W = \frac{1}{2}(1+\tau)^{1/\tau}\, C_W .$$

emulate Pauli blocking via effective potential

$$V_{\rm Pauli} = \frac{C_{\rm P}}{2} \left(\frac{1}{q_0 p_0}\right)^3 \sum_{i,j(\neq i)} \exp\left[-\frac{(\mathbf{R}_i-\mathbf{R}_j)^2}{2q_0^2} - \frac{(\mathbf{P}_i-\mathbf{P}_j)^2}{2p_0^2}\right] \delta_{\tau_i\tau_j}\delta_{\sigma_i\sigma_j}$$

momentum dependent and isospin part

$$V_{\mathrm{MD}} = \frac{C_{\mathrm{ex}}^{(1)}}{2\rho_0} \sum_{i,j(\neq i)} \frac{1}{1+\left[\frac{\mathbf{P}_i-\mathbf{P}_j}{\mu_1}\right]^2} \rho_{ij} + \frac{C_{\mathrm{ex}}^{(2)}}{2\rho_0} \sum_{i,j(\neq i)} \frac{1}{1+\left[\frac{\mathbf{P}_i-\mathbf{P}_j}{\mu_2}\right]^2} \rho_{ij} ,$$

$$V_{\mathrm{Coul}} = \frac{e^2}{2} \sum_{i,j(\neq i)} \left(\tau_i + \frac{1}{2}\right) \left(\tau_j + \frac{1}{2}\right) \iint d^3\mathbf{r}\, d^3\mathbf{r}' \frac{1}{|\mathbf{r}-\mathbf{r}'|} \rho_i(\mathbf{r})\rho_j(\mathbf{r}') ,$$

Isospin $\tau = \pm 1/2$

$$V_{\mathrm{sym}} = \frac{C_{\mathrm{s}}^{(1)}}{2\rho_0} \sum_{i,j(\neq i)} (1-2|\tau_i-\tau_j|)\, \rho_{ij}$$

$$+\frac{C_{\mathrm{s}}^{(2)}}{(1+\gamma)\rho_0^{\gamma}} \sum_i \left[\sum_{j(\neq i)} (1-2|\tau_i-\tau_j|)\, \rho_{ij}\right]^{\gamma}$$

non-linear isospin interactions (like Skyrme)

parameter set from Maruyama et al, PRC 57, 655
as starting point of investigation

solving equations of motion

including damping or coupling to a heat bath (Nosé-Hoover)

QMD equations with frictional terms:

$$\dot{\mathbf{R}}_\mathbf{i} = \frac{\partial H}{\partial \mathbf{P}_\mathbf{i}} - \mu_R \frac{\partial H}{\partial \mathbf{R}_\mathbf{i}},$$

$$\dot{\mathbf{P}}_\mathbf{i} = -\frac{\partial H}{\partial \mathbf{R}_\mathbf{i}} - \mu_P \frac{\partial H}{\partial \mathbf{P}_\mathbf{i}},$$

$$\mu_R\,, \mu_P > 0 \quad \text{and} \quad \ll 1$$

predictor-corrector and adaptive time step

computational comparison GPU to CPU

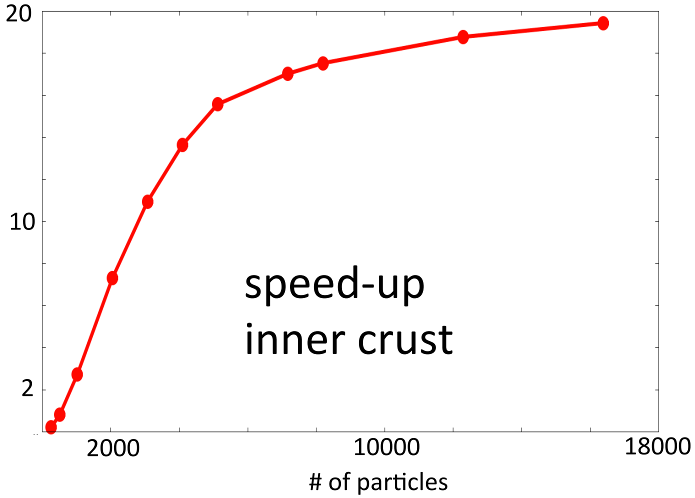

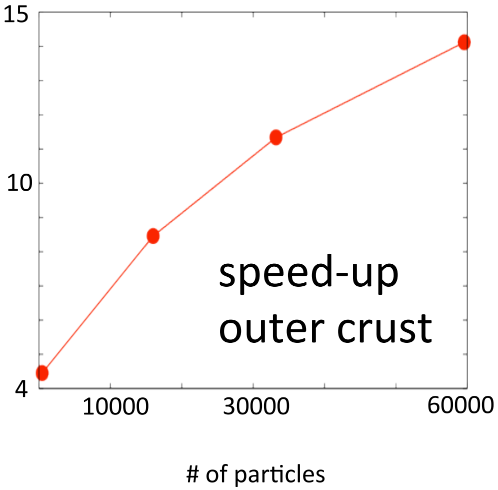

LOEWE-CSC Frankfurt

architecture: dual-CPU with total of 24 cores

total of 800 GPU cards
About 1800 cores per GPU
larger system upgrade in preparation

Substantial speed up (however, CPU version not optimized!)

work on multi-GPU and CPU+GPU versions continuing

Taylor expansion in isospin-related quantities

simulate at different densities and isospin
determine Taylor coefficients

$$e(\rho, \delta) = e_0(\rho) + e_{\mathrm{sym}}(\rho)\delta^2$$

slope $$L = 3\rho_0 \frac{\partial e_{\mathrm{sym}}(\rho)}{\partial \rho}\bigg|_{\rho=\rho_0}$$

numerically $$L = 3\rho_0 \frac{e_{\mathrm{sym}}(1.1\rho_0) - e_{\mathrm{sym}}(0.9\rho_0)}{1.1\rho_0 - 0.9\rho_0}$$

Saturation density as function of isospin asymmetry $\delta = (\rho_p - \rho_n) / (\rho_p + \rho_n)$

lowest order $$\frac{\rho_s}{\rho_0} = 1 - \frac{3L}{K_0}\delta^2$$

Binding energy per particle (without Coulomb)

Set	$C_s^{(1)}$(MeV)	$C_s^{(2)}$(MeV)	γ	$E_{\rm sy}(\rho_0)$(MeV)	L(MeV)
I	30.0	−15.0	3.0	34.7	79.0
II	25.0	0.0	0.0	34.6	94.3
III	18.0	22.5	3.0	34.7	117.9

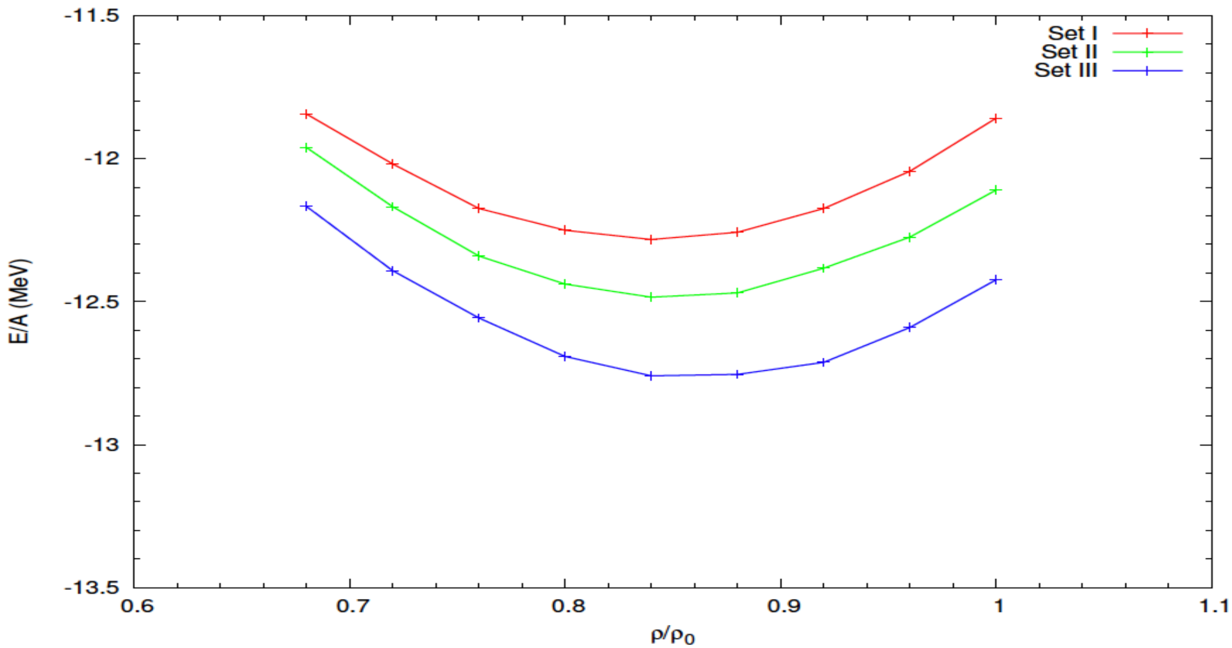

$Y_p = 0.31$

saturation densities change slightly

agrees with $$\frac{\rho_s}{\rho_0} = 1 - \frac{3L}{K_0}\delta^2 - \frac{3L_{\rm sym,4}}{K_0}\delta^4$$

isospin dependence of binding energy

results for different baryon densities

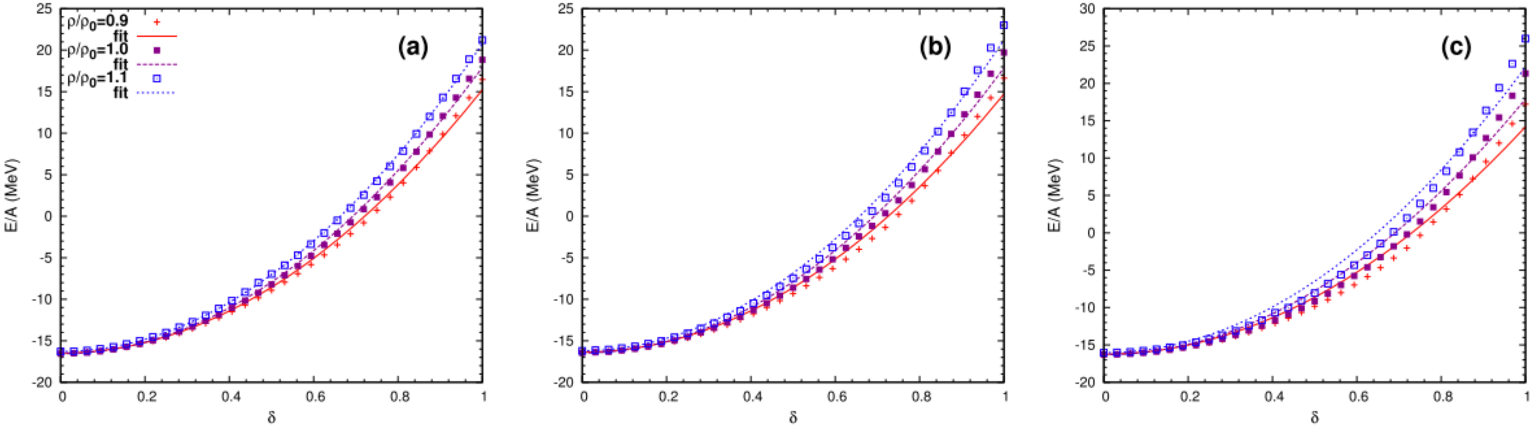

4^{th} order fit in δ :

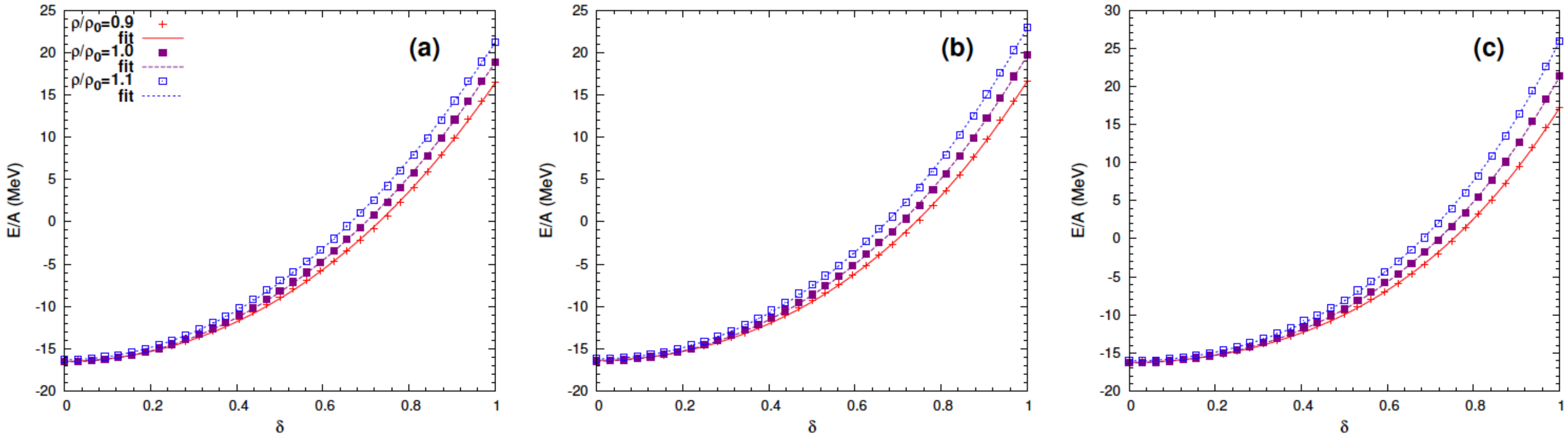

Nandi, SWS, arXiv:1601.01842

testing ordinary nuclei

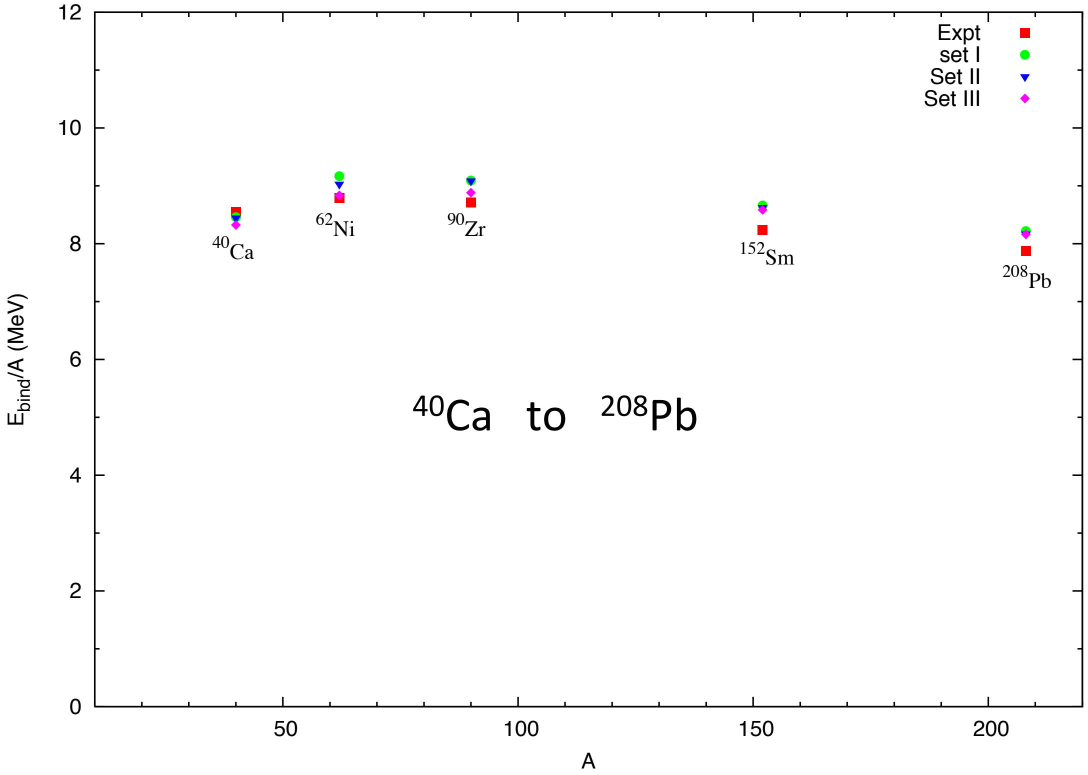

works fine for all parameterizations

also relevant for HI collisions (fragmentation)

importance of pasta phase

Properties of the pasta phase are of importance to neutron stars and core-collapse supernovae

- Neutrino-pasta scattering is crucial in neutrino transport in core collapse supernova (Horowitz et al., PRC69, 045804)
- e^- - pasta scattering is important to determine a number of transport properties, like shear viscosity, thermal conductiviy, electrical conductivity (Horowitz et al., PRC78, 035806)
- Electrical conductivity of the pasta has strong impact on decay of neutron star magnetic fields (Pons et al, Nature Phys. 9, 431)
- Relates to crustal oscillations, pulsar glitches, cooling, …

Pasta phases

Properties of pasta phase largely studied with static methods:

liquid-drop model, Thomas-Fermi, Hartree-Fock, …

Models assume few specific shapes and obtain favouralble shape by minimozing free energy.

The phase diagram possesses a universal basic feature
With increasing density the shape of the nuclear matter region changes like

sphere → cylinder → slab → cylindrical hole → spherical hole → uniform

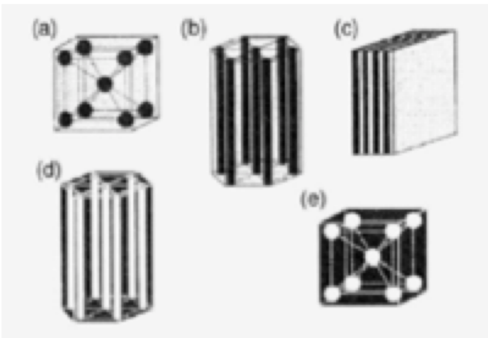

from Oyamatsu (1993)

there might be many complex structures

shapes in the crust

4 Minkowski functionals to describe shapes in 3 dimensions:

volume V surface area S plus

mean curvature

$$H = \frac{1}{2} \int_{\partial K} (\kappa_1 + \kappa_2) dA$$

Euler characteristics

$$\chi = \frac{1}{2\pi} \int_{\partial K} \kappa_1 \cdot \kappa_2 \, dA$$

non-trivial numerical task – define surface ∂K

subdivide volume into voxels, calculate densities
create polygonal surface, determine functionals

requires testing invariance of results with changing definition various structures and characteristics

Sphere $\Rightarrow$ $H > 0,\ \chi > 0$

Cylinder $\Rightarrow$ $H > 0,\ \chi = 0$

Slab: $\Rightarrow$ $H = 0,\ \chi = 0$

Cylindrical hole $\Rightarrow$ $H < 0,\ \chi = 0$

Spherical hole $\Rightarrow$ $H < 0,\ \chi > 0$

snapshots from molecular dynamics runs

$0.1\ \rho_0$

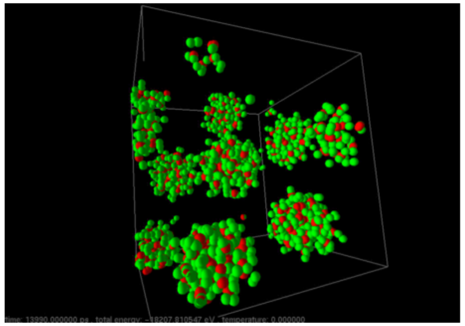

$0.225\ \rho_0$

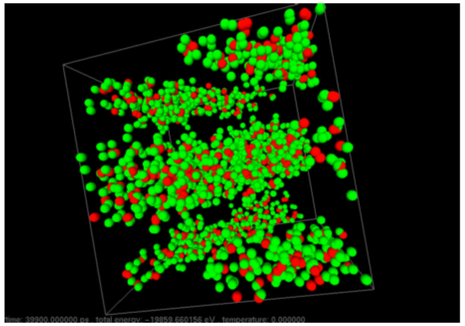

$0.36\ \rho_0$

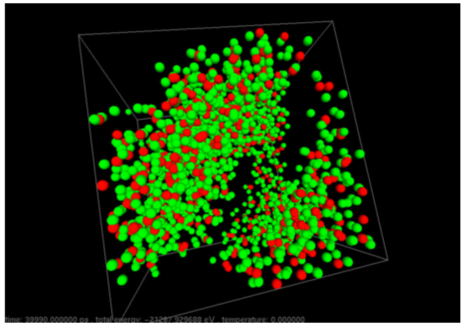

$0.45\ \rho_0$

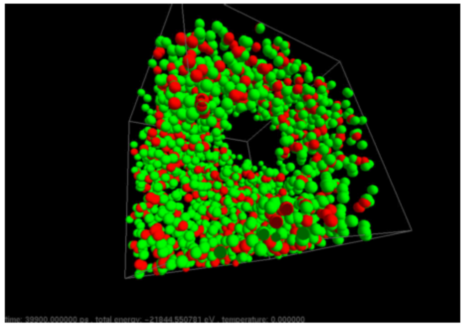

$0.5\ \rho_0$

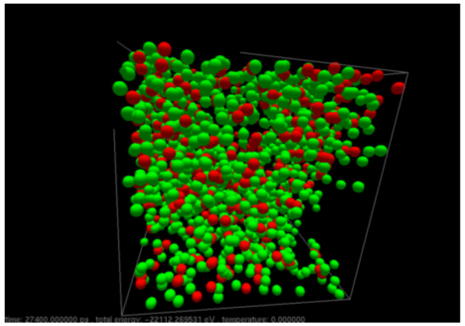

structures for different densities at fixed proton to neutron ratio $Y_p = 0.31$ relevant for supernova simulations

Minkowsi functionals

define inside / outside of nuclear structures

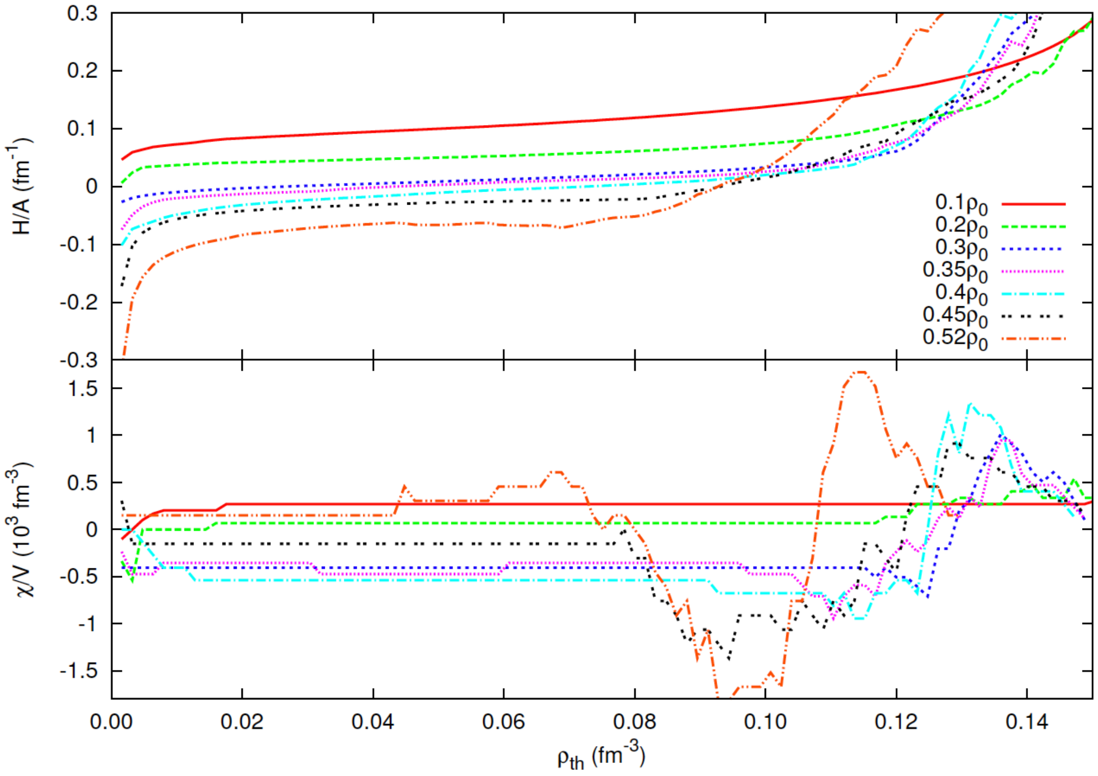

threshold density

Isospin quantities and potential relevance for pasta

Symmetry energy at saturation is reasonably constrained at saturation to be around E_{sym} ~ 32 MeV

Slope of the symmetry energy L, i. e. the change of its value with density is far more uncertain with L ~ 20 – 120 MeV.

Recent static calculations (Grill et al, PRC 85, 0555808 (2012), Bao et al, PRC 89, 045807 (2014)) find that L might have dramatic effects on pasta structures.
For some models pasta phase vanishes completely if L has high value.

Motivation to study effect of symmetry energy and slope on the pasta phase with the dynamic model

Minkowski functionals for symmetric matter

mean curvature

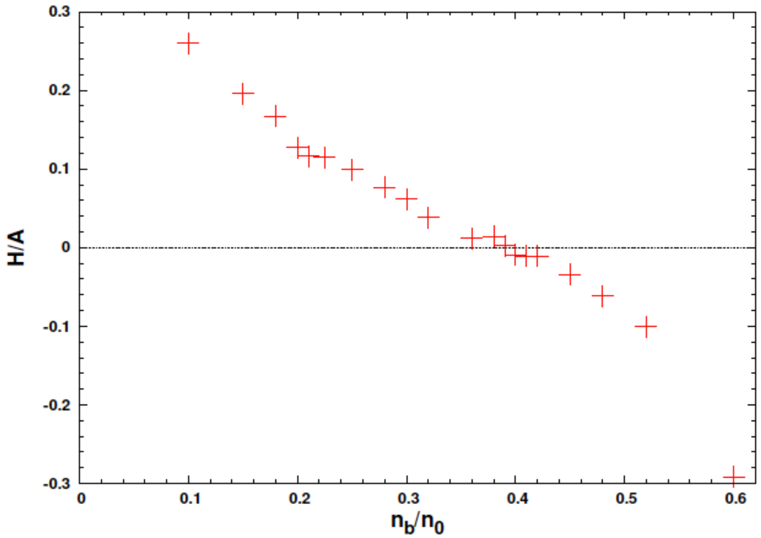

Gaussian curvature

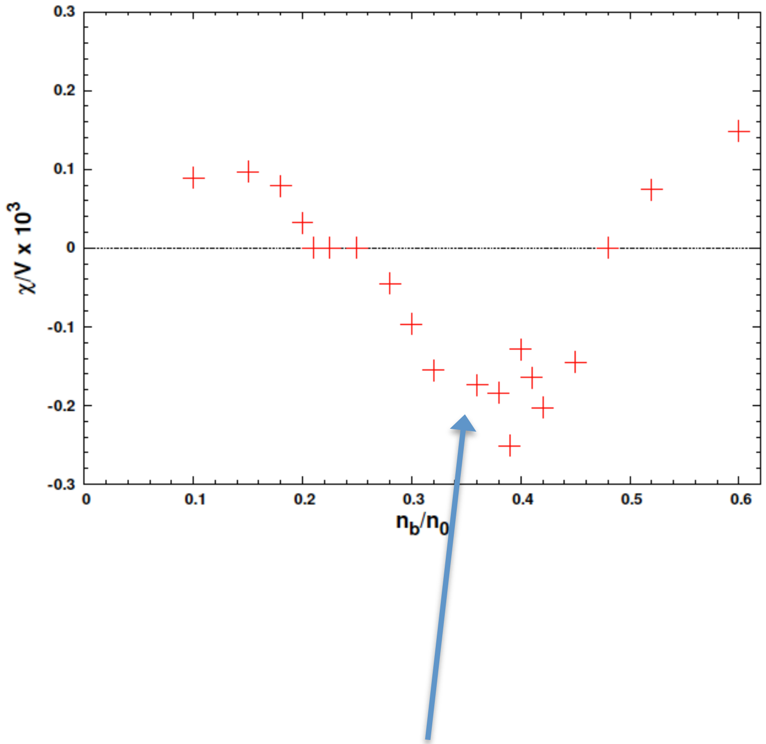

X = number of isolated regions + number of cavities – number of tunnels

Density dependence of Minkowski functionals

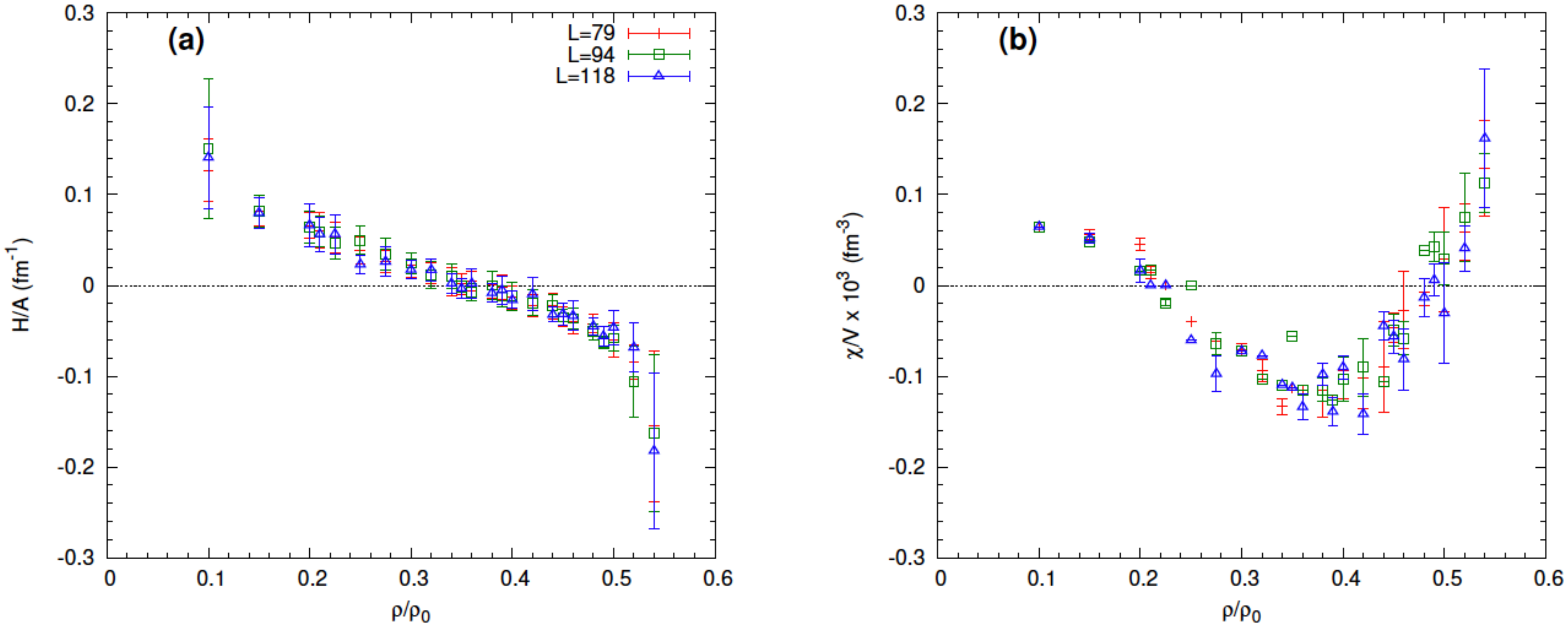

results for different slope L show small change

observed range of pasta phase between ~ 0.1 ρ_0 and 0.55-0.6 ρ_0
largely independent of L

fluctuations of different particles / slopes and densities

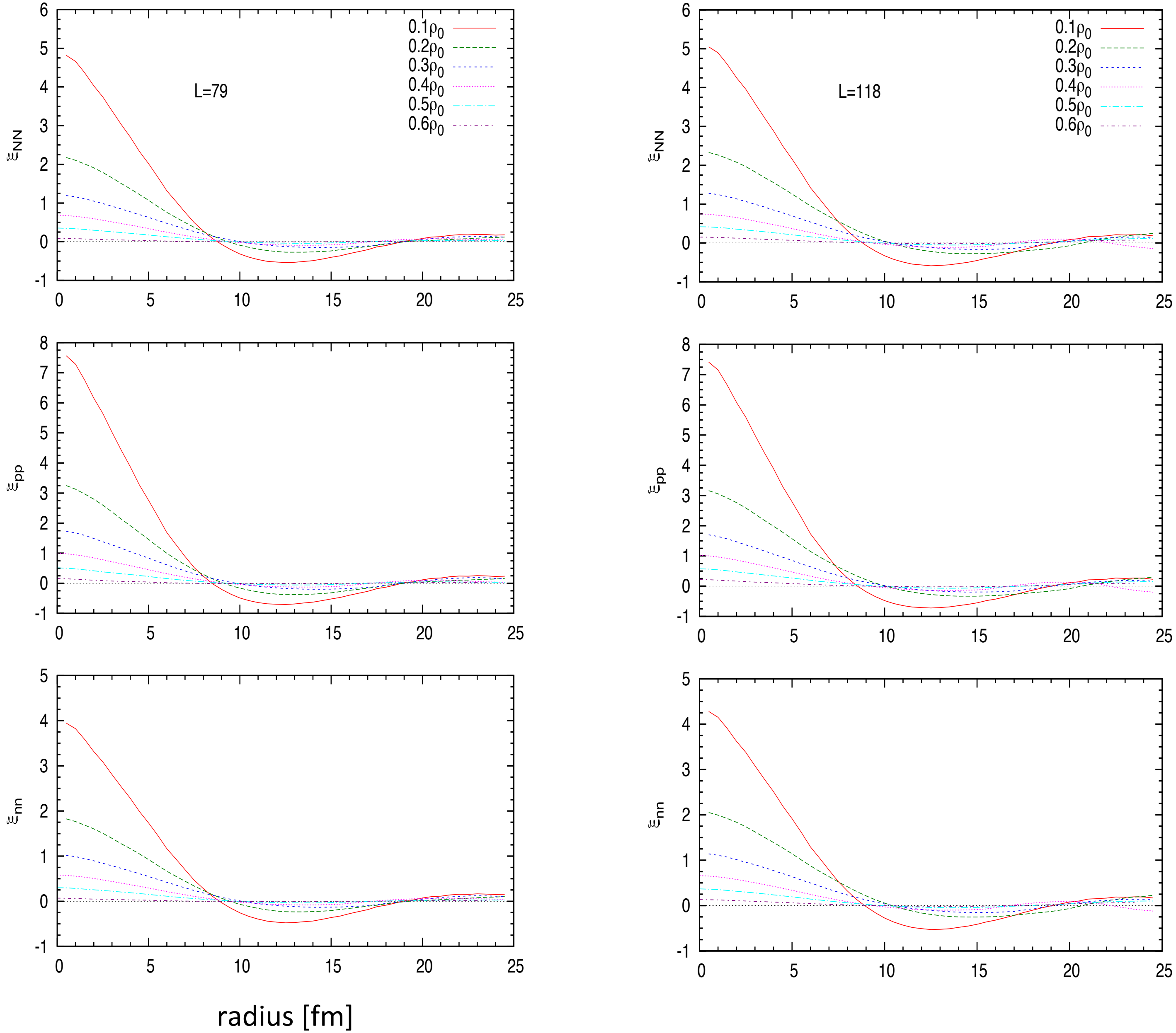

zoom into transition region

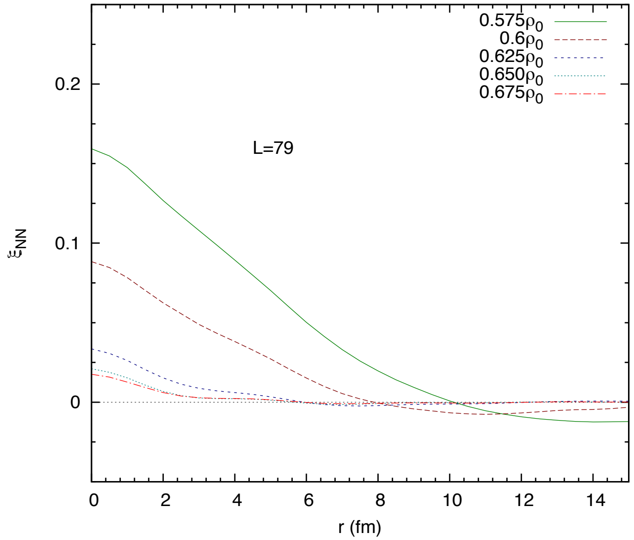

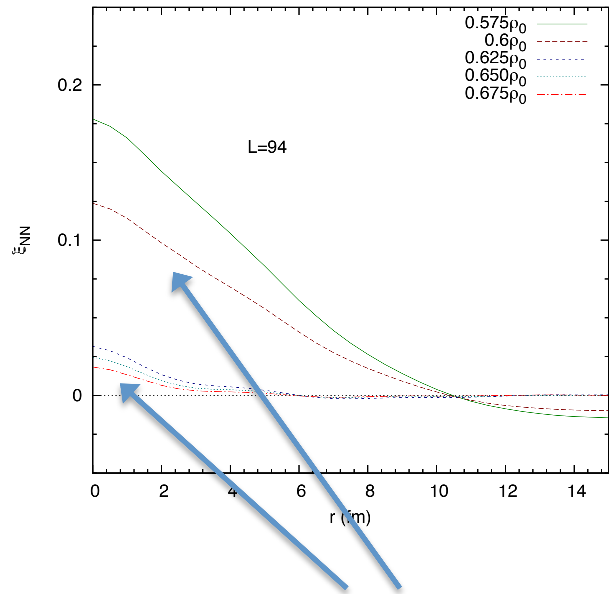

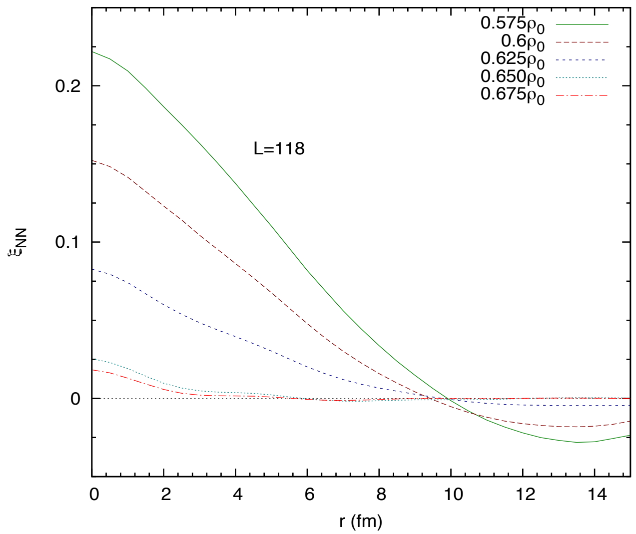

crust-core transition

transition density not strongly dependent on slope

fast transition   in contrast to Watanabe et al (2006)

look at liquid-gas (heavy-ions)

Conclusions, Outlook

- Developed efficient code for outer and inner crust
- Good description of ground state nuclear matter / nuclei
- As first step – use established interaction / extend to study isospin effects
- Overall pasta phases, relevant densities largely insensitive to isospin

Next steps:

Calculate transport properties
Different interactions
Pycnonuclear reactions
Use in heavy-ion simulations
Extend code to mixed CPU/GPU version

many thanks to the organizers!

FIAS Frankfurt Institute for Advanced Studies
NAVI
HIC for FAIR Helmholtz International Center

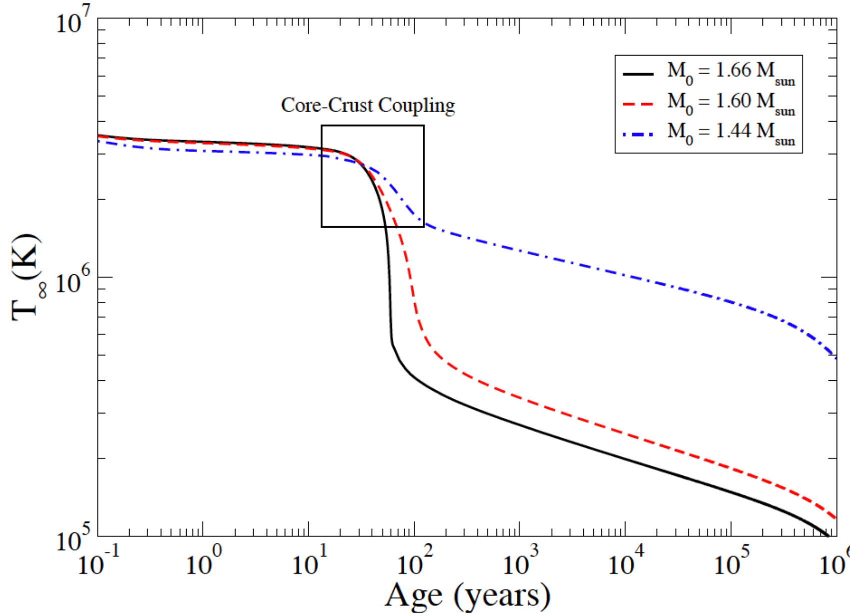

Core-Crust Coupling
M_0 = 1.66 M_{sun}
M_0 = 1.60 M_{sun}
M_0 = 1.44 M_{sun}
T_∞ (K)
Age (years)
10^7
10^6
10^5
10^{-1}
10^0
10^1
10^2
10^3
10^4
10^5
10^6

energy per particle as function of proton fraction

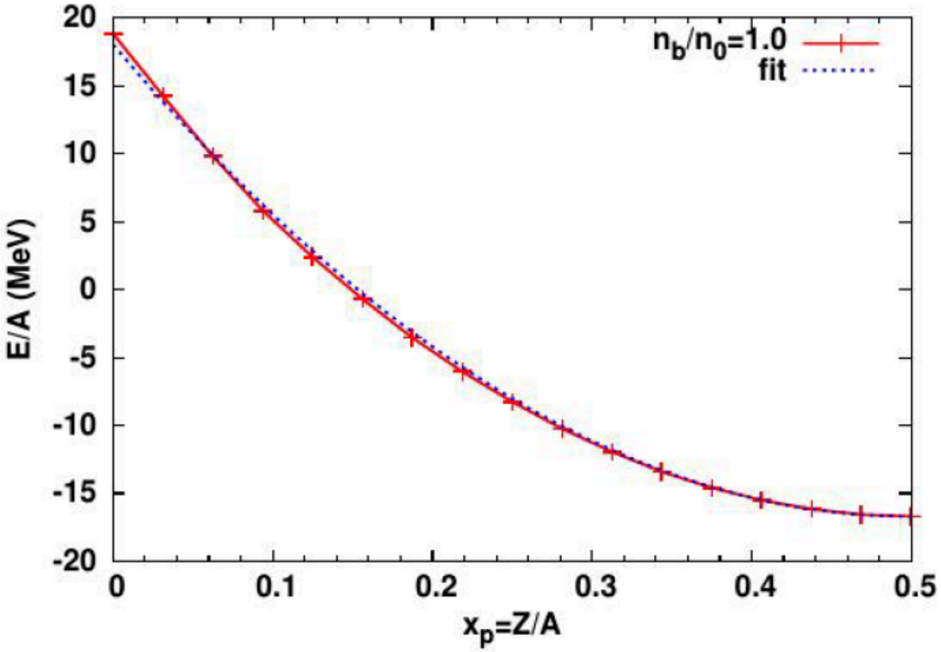

calculate slope

$$L = 3\rho_0 \frac{dE_{\rm sy}}{d\rho}\bigg|_{\rm sat} = 3\rho_0 \frac{E_{\rm sy}(1.1\rho_0) - E_{\rm sy}(0.9\rho_0)}{1.1\rho_0 - 0.9\rho_0}$$

Taylor expansion in isospin-related quantities

simulate at different densities and isospin
with extended Taylor expansion (be careful with simple approximations)

$$e(\rho, \delta) = e_0(\rho) + e_{\mathrm{sym}}(\rho)\delta^2 + e_{\mathrm{sym},4}(\rho)\delta^4$$

$$L = 3\rho_0 \frac{\partial e_{\mathrm{sym}}(\rho)}{\partial \rho}\bigg|_{\rho=\rho_0} \qquad L_{\mathrm{sym},4} = 3\rho_0 \frac{\partial e_{\mathrm{sym},4}(\rho)}{\partial \rho}\bigg|_{\rho=\rho_0}$$

$$e_{\mathrm{sym},4}(\rho) = e_{\mathrm{sym},4}(\rho_0) + L_{\mathrm{sym},4}\chi$$

Saturation density as function of isospin asymmetry $\delta = (\rho_p - \rho_n) / (\rho_p + \rho_n)$

$$\frac{\rho_s}{\rho_0} = 1 - \frac{3L}{K_0}\delta^2 - \frac{3L_{\mathrm{sym},4}}{K_0}\delta^4$$